

Theoretical and Experimental Investigation of the Thermochemistry of $\text{CrO}_2(\text{OH})_2(\text{g})$

Elizabeth J. Opila,* Dwight L. Myers,† Nathan S. Jacobson, Ida M. B. Nielsen,‡
Dereck F. Johnson, Jami K. Olminsky,§ and Mark D. Allendorf‡

NASA Glenn Research Center, Cleveland, Ohio 44135-3191, East Central University,
Ada, Oklahoma 74820-0689, Sandia National Laboratories, Livermore, California 94551-0969, and
QSS Group, Inc., NASA Glenn Research Center, Cleveland, Ohio 44135-3191

Received: July 25, 2006; In Final Form: December 22, 2006

In this paper, we report the results of equilibrium pressure measurements designed to identify the volatile species in the Cr–O–H system and to resolve some of the discrepancies in existing experimental data. In addition, ab initio calculations were performed to lend confidence to a theoretical approach for predicting the thermochemistry of chromium-containing compounds. Equilibrium pressure data for $\text{CrO}_2(\text{OH})_2$ were measured by the transpiration technique for the reaction $0.5\text{Cr}_2\text{O}_3(\text{s}) + 0.75\text{O}_2(\text{g}) + \text{H}_2\text{O}(\text{g}) = \text{CrO}_2(\text{OH})_2(\text{g})$ over a temperature range of 573 to 1173 K at 1 bar total pressure. Inductively coupled plasma atomic emission spectroscopy (ICP-AES) was used to analyze the condensate in order to quantify the concentration of Cr-containing volatile species. The resulting experimentally measured thermodynamic functions are compared to those computed using B3LYP density functional theory and the coupled-cluster singles and doubles method with a perturbative correction for connected triple substitutions [CCSD(T)].

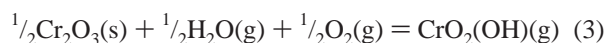
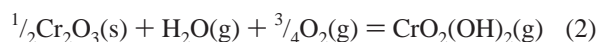
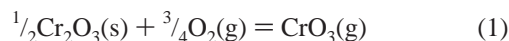
Introduction

The corrosion of chromium-containing materials in oxidizing environments via the formation of volatile species is a problem with both broad technological and environmental implications. Chromium in the +6 valence state is considered to be a carcinogenic hazard of special concern in waste incineration processes.¹ In addition, loss of chromium in the presence of air and water vapor is a major technological roadblock in the development of solid oxide fuel cells, which use chromia-forming alloys or conductive chromia-containing ceramics as interconnects.^{2,3} Deposition of chromium oxides on catalysts used in steam-methane reformers leads to substantial reductions in catalyst lifetimes.⁴ Furthermore, lifetimes of Cr-rich structural steels used in oxygen- and steam-containing environments are reduced due to chromia volatility.^{5,6} Finally, volatile chromium-containing species formed in atmospheric pressure chemical vapor deposition reactors used in the semiconductor industry can contaminate processed wafers, causing increased defect rates.⁷

A large number of gas-phase Cr–O–H species could potentially be involved in these degradation processes, for which little experimentally measured thermodynamic data are available. Several systematic theoretical examinations of the Cr–O–H system have been conducted. In an important study, Ebbinghaus derived thermodynamic data for a large number of gas-phase chromium oxides and oxyhydroxides using a combination of the limited available experimental data and the molecular constant method.¹ Empirical relationships were employed, where needed, to estimate unknown molecular properties, resulting in large uncertainties in some cases. Later, Espelid et al.⁸ used high-level ab initio calculations to predict equilibrium geometries and vibrational frequencies (using B3LYP) and electronic

energies (using the coupled cluster CCSD(T) method with the PCI-X extrapolation scheme and G2 calculations), from which they derived heats of formation for a number of gas-phase chromium oxides and oxyhydroxides. In several cases, the predicted values differ from those of Ebbinghaus by more than 30 kJ mol⁻¹. There is thus a critical need for new experimental data to resolve inconsistencies between theory and published data, as well as to validate computational methods that are the only practical means of generating thermodynamic properties across the large range of molecules that are possible in this system.

The volatile species CrO_3 ,^{9–12} $\text{CrO}_2(\text{OH})_2$,¹³ and $\text{CrO}_2(\text{OH})^{12}$ have all been experimentally identified as contributing to Cr_2O_3 degradation. The reactions to form these volatile Cr–O–H species from Cr_2O_3 , H_2O , and O_2 are as follows:



Ebbinghaus concluded from equilibrium calculations using his estimated data that $\text{CrO}_2(\text{OH})_2(\text{g})$ is the dominant vapor species above chromium-containing materials exposed to oxygen and water vapor across a wide range of temperatures, as shown in Figure 1. However, the identity of the volatile species formed in water vapor–oxygen mixtures at temperatures between 573 and 1173 K has not been definitively established with experiments. Both $\text{CrO}_2(\text{OH})_2^+$ and $\text{CrO}_2(\text{OH})^+$ ions were observed in earlier mass spectrometry experiments conducted at 1373 K.^{13,14} It is uncertain whether both gas species were formed by reaction of water vapor and oxygen with $\text{Cr}_2\text{O}_3(\text{s})$ or whether $\text{CrO}_2(\text{OH})^+$ was formed as a fragment during the ionization of $\text{CrO}_2(\text{OH})_2$. In addition, Kim and Belton¹² studied the volatilization of $\text{Cr}_2\text{O}_3(\text{s})$ in oxygen and water vapor in the temperature

* Corresponding author. E-mail: opila@nasa.gov.

† East Central University.

‡ Sandia National Laboratories.

§ QSS Group, Inc..

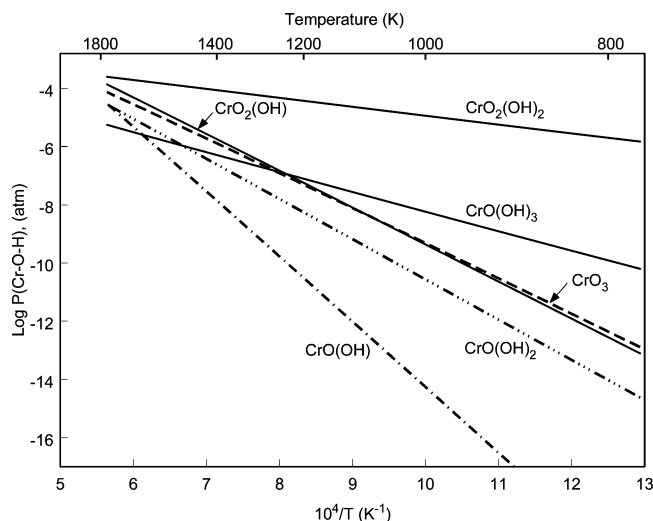


Figure 1. Equilibrium partial pressures of volatile Cr–O–H species calculated at $P(\text{H}_2\text{O}) = 0.5$ bar and $P(\text{O}_2) = 0.5$ bar based on the data of Ebbinghaus.¹

TABLE 1: Literature Values for the Standard Heat of Formation, $\Delta H_{f,298}^\circ$, $\text{Cr}(\text{s}) + 2\text{O}_2(\text{g}) + \text{H}_2(\text{g}) = \text{CrO}_2(\text{OH})_2(\text{g})$

study	method	$\Delta H_{f,298}^\circ$ (kJ mol ⁻¹)
IVTANTHERMO ¹⁶	estimation based on like molecules	-736 ± 40
Farber & Srivastava ¹⁴	mass spectrometry measurements	-738 ± 29
Ebbinghaus ¹	estimation based on ref 15	-748 ± 4.3
Espelid ⁸	average, ab initio calculation	-787 ± 36
	G2(MP2/CC)	-812
	PCI-X	-762

range of 1572 to 1798 K and found pressure-dependent results consistent with $\text{CrO}_2(\text{OH})(\text{g})$ formation. Glemser and Müller¹⁵ obtained equilibrium pressure results for $\text{CrO}_2(\text{OH})_2(\text{g})$ from a different reaction



at much lower temperatures, between 408 and 458 K. Clearly, the unambiguous identification of the dominant Cr–O–H(g) species formed in environments and at temperatures of technological interest is still needed.

Although it is generally assumed that $\text{CrO}_2(\text{OH})_2(\text{g})$ is the species formed under conditions of practical interest, the available standard heats of formation for this species vary widely and have high degrees of uncertainty, as summarized in Table 1. The data in the IVTANTHERMO database¹⁶ were estimated in 1985 and are based on estimated molecular parameters (geometry and vibrational frequencies) and enthalpies of formation derived by comparison of $\text{CrO}_x(\text{OH})_y$ with corresponding CrO_xF_y species.¹⁷ At the time of Ebbinghaus' assessment of the Cr–O–H system, the only experimental data available for analysis were those of Farber and Srivastava¹⁴ and Glemser and Müller.¹⁵ Ebbinghaus rejected the Farber and Srivastava data, which were derived from mass spectrometric measurements, due to possible interference from chromium oxychloride species. The data of Glemser and Müller¹⁵ led Ebbinghaus to estimate the uncertainty in his reported heat of formation to be only ±4.3 kJ mol⁻¹. Experimental equilibrium pressure data for $\text{CrO}_2(\text{OH})_2(\text{g})$ are now available from several sources,^{18–20} and these newer data do not agree with the equilibrium predictions of Ebbinghaus.¹ Unfortunately, standard heats of formation are not reported in these studies for comparison with the earlier data. The recent theoretical results of Espelid⁸ do not clarify the

TABLE 2: Thermochemical Data (kJ mol⁻¹) from the Literature Employed in the Computation of the Heat of Formation for $\text{CrO}_2(\text{OH})_2$

	$\Delta H_{f,0}^\circ$	$\Delta H_{f,298.15}^\circ$
$\text{H}_2\text{O}(\text{g})$	-238.921 ± 0.042 ^a	-241.826 ± 0.042 ^a
$\text{CrO}_3(\text{g})$	-319.5 ± 4.2 ^b	-323.5 ± 4.2 ^c

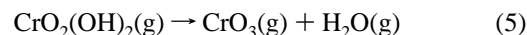
^a Reference 21. ^b Computed from the reaction $\text{Cr}(\text{s}) + 1.5\text{O}_2(\text{g}) \rightarrow \text{CrO}_3(\text{g})$ using the $\Delta H_{f,298.15}^\circ[\text{CrO}_3]$ value and the enthalpy differences $H_{298.15}^\circ - H_0^\circ$ for Cr(s), $\text{O}_2(\text{g})$, and $\text{CrO}_3(\text{g})$ given in ref 1. ^c From ref 1.

situation because their heats of formation predicted by the G2 and PCI(X) methods differ by 50 kJ mol⁻¹. Thus, for both scientific and practical reasons, there is strong justification for performing a concentrated investigation of the thermochemistry of $\text{CrO}_2(\text{OH})_2$.

The objectives of this work are to experimentally verify that $\text{CrO}_2(\text{OH})_2(\text{g})$ is the dominant volatile Cr–O–H species for Cr_2O_3 exposed in H_2O and O_2 at temperatures between 573 and 1173 K, to obtain reliable thermodynamic data for $\text{CrO}_2(\text{OH})_2(\text{g})$ using both the transpiration technique and ab initio calculations, to compare experimental data to calculated data, and to clarify the importance of other volatile species in the Cr–O–H system.

Theoretical Calculations

The heat of formation for $\text{CrO}_2(\text{OH})_2$ was computed from the isogyric reaction



The reaction energy was first computed at 0 K and then converted to a reaction energy at 298.15 K by application of temperature corrections

$$\Delta H_{r,298.15}^\circ = \Delta H_{r,0}^\circ + H_{\text{Thermal}}^\circ(\text{CrO}_3) + H_{\text{Thermal}}^\circ(\text{H}_2\text{O}) - H_{\text{Thermal}}^\circ(\text{CrO}_2(\text{OH})_2) \quad (6)$$

where $H_{\text{Thermal}}^\circ = H_{298.15}^\circ - H_0^\circ$. The heat of formation was then obtained from the expression

$$\Delta H_{f,T}^\circ(\text{CrO}_2(\text{OH})_2) = \Delta H_{f,T}^\circ(\text{CrO}_3) + \Delta H_{f,T}^\circ(\text{H}_2\text{O}) - \Delta H_{r,T}^\circ \quad (7)$$

for $T = 0$ K and $T = 298.15$ K, using the literature values for the heats of formation of $\text{CrO}_3(\text{g})$ and $\text{H}_2\text{O}(\text{g})$ listed in Table 2. Although conflicting data for the heat of formation of $\text{CrO}_3(\text{g})$ are found in the literature,^{1,12,16,21} the value provided by Ebbinghaus has the highest degree of accuracy for any Cr–O vapor-phase species. This point is addressed further in a discussion of $\text{CrO}_3(\text{g})$ stability in a later section of this paper.

Geometries and harmonic vibrational frequencies for the participating species were computed using the B3LYP density functional method with the 6-311++G(d,p) basis set,^{22–25} which is of triple- ζ quality and includes diffuse and polarization functions on all atoms. Using the B3LYP/6-311++G(d,p) geometries, the reaction energy was computed with the coupled-cluster singles and doubles method with a perturbative correction for connected triple substitutions [CCSD(T)] employing the frozen-core approximation (freezing 1s on O and 1s2s2p3s3p on Cr). For the coupled-cluster computations, the Bauschlicher ANO basis set^{26,27} was used on Cr, and for H and O the cc-pVTZ basis²⁸ was employed.

The effect of inclusion of the chromium 3s and 3p core orbitals in the correlation procedure was computed using second-

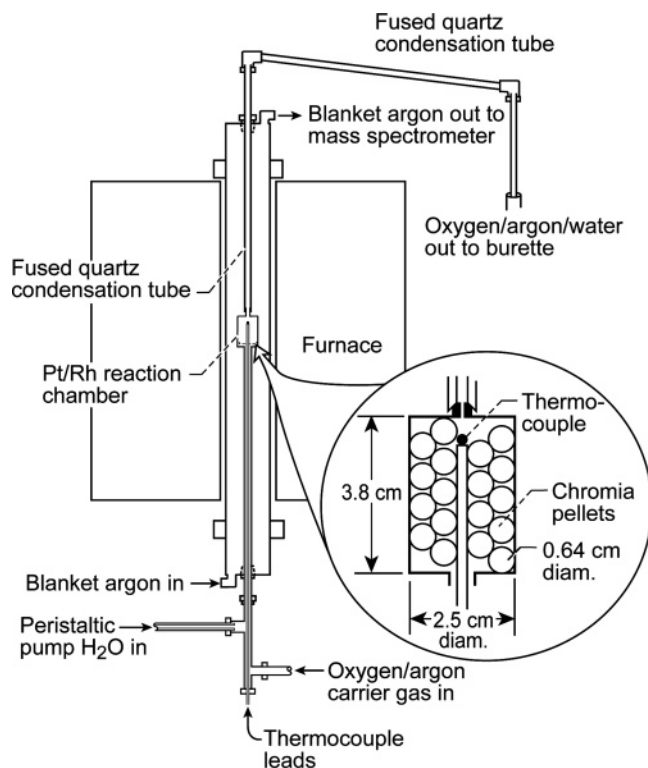


Figure 2. Schematic drawing of the transpiration equipment.

order Møller–Plesset perturbation (MP2) theory in conjunction with the cc-pVTZ basis for H and O and a modified Bauschlicher ANO set for Cr. The Bauschlicher ANO basis set was modified by decontracting the outermost six s, seven p, and seven d functions. A correction for basis-set incompleteness was estimated by computation of large-basis-set MP2 energies using a completely decontracted Bauschlicher ANO basis set on Cr and the aug-cc-pVQZ set^{28,29} on H and O. Scalar relativistic effects were accounted for at the MP2 level using the Douglas–Kroll–Hess second-order relativistic correction.^{30–33} For Cr, the Bauschlicher ANO set, modified by decontracting the entire s and p spaces, was employed, and the cc-pVTZ_DK set^{27,34} was used for H and O. Temperature corrections $H_{298.15}^0 - H_0^0$ were computed using the B3LYP/6-311++G(d,p) harmonic vibrational frequencies, employing standard formulas from statistical mechanics³⁵ and including a hindered rotor treatment³⁶ of the vibrational modes corresponding to internal rotation of the hydroxide groups.

The relativistic corrections were computed with NWChem,³⁷ the large basis set MP2 computations were carried out with MPQC,³⁸ and other computations were performed with the Gaussian03 program.³⁹

Experimental Materials and Methods

Material. The Cr_2O_3 used for experiments was –20 mesh powder with a reported purity of 99.997% (Cerac, Milwaukee, WI). The impurity content was measured by DC arc emission spectroscopy and found to be 0.011% Bi, 0.001% Ca, 0.0006% Si, and 0.008% Ti. The powder was cold pressed at 14 MPa with a 0.64-cm-diameter die using water as a binder. The pellets were partially sintered for 4 h in air at 1633 K, resulting in a density of approximately 60% of the theoretical value.

Transpiration Technique. The transpiration technique is a well-established and versatile technique for studying gas–solid equilibria and measuring equilibrium pressures in the presence of large concentrations of other gases.⁴⁰ Figure 2 shows a

schematic drawing of the transpiration setup used in these experiments. The reactive gases, oxygen and water vapor, as well as a nonreactive carrier gas, argon, flowed over the Cr_2O_3 pellets that were contained in a Pt-20Rh reaction cell. Flow rates were chosen to eliminate any diffusion effects or kinetic limitations so that the equilibrium pressure of volatile Cr–O–H species was established in the reaction chamber. Volatile species flowed into the cooler fused quartz tubes and condensed along with the water vapor. The deposits as well as the water were collected and quantitatively analyzed for Cr. Knowing the moles of oxygen and water vapor input as well as the moles of Cr collected, the equilibrium constant for the volatility reaction was determined.

The following precautions were taken to ensure accurate data determination. The gas inlet was constricted by the thermocouple tube while the outlet was constricted by a small-diameter hole in the upper Pt-20Rh plug to maintain equilibrium in the cell. The inner diameter of the bottom of the vertical fused quartz condensation tube was beveled by grinding with diamond tools. This bevel was pressure fit to the Pt-20Rh outlet of the transpiration cell. The horizontal fused quartz condensation tubes were connected to the vertical tube with polyfluoroethylene fittings to avoid the introduction of chromium into the system through stainless-steel fittings. Following tube assembly and prior to each experiment, the tube end at the water collection burette was briefly sealed while inlet gases flowed into the cell until pressures of at least 1.33 bar (1000 Torr) were measured with the capacitance manometer. This test was used to verify that the tubing assembly did not leak. The pressure was then released, and the inlet water flow was initiated. The experimental time was measured from the start of the inlet water flow to the time when the water flow was terminated. Water that flowed through the transpiration system was collected and measured in a burette. The amount of water collected was within 5% of the calculated total throughput corrected for the amount of water expected to be lost to vaporization at room temperature. The assembly was again tested for leak-tightness after each experiment before disassembling the collection tubes. The condensate in all collection tubes, as well as the collected water, was analyzed for Cr content as described below. It was critical to collect and analyze the deposit from the entire gas train. Prior to and after each experiment, the liquid water flow for the inlet was calibrated by flowing into a burette or graduated cylinder. Water flow rates obtained before and after an experiment were, on average, constant within 0.06 mL/hr. During each experiment, the portion of the vertical collection tube outside of the furnace and the initial portion of the horizontal collection tube were wrapped with heating tape to ensure that water did not condense and flow back into the vertical tube. The transpiration cell and gas train were enclosed in a furnace tube that contained a blanket of flowing argon. The argon limited the formation of $\text{PtO}_2(\text{g})$ from the transpiration cell. In addition, the blanket argon was analyzed for oxygen and water vapor using a residual gas analyzer (Dycor/Ametek, Pittsburgh, PA) to detect any leaks from the transpiration gas train system.

Experimental Conditions. Chromia volatility was measured over a temperature range of 573 to 1173 K. Temperature measurements were made with a Type-R thermocouple immersed in the chromia pellets as shown in the detail of Figure 2. The thermocouple was periodically calibrated with a NIST traceable thermocouple and found to be within 5 K of the standard. The experiments were conducted at ambient pressure. The transpiration cell pressure was monitored with a capacitance monitor and varied between 0.93 and 1.02 bar (695 to 762 Torr)

during the course of these experiments. The pressure measured with the capacitance monitor was found to vary with ambient conditions and was within 0.3% of a nearby barometric standard.⁴¹ The temperature- and pressure-dependent experiments were conducted with the total cell flow rates (argon, oxygen, water vapor, volatile chromium species) between 7.55 and 17.04 mL/s at the experimental temperature. Inlet liquid water flow rates were controlled with a peristaltic pump (Rainin, Instrument Co., Woburn, MA) and varied between 0.33 and 6.80 mL/h. Water vapor contents in the cell varied between 4% and 48% of the total flow. Inlet oxygen flow rates varied between 50 and 471 sccm. Oxygen contents in the cell varied between 13% and 100% of the total flow. Inlet argon flow rates varied between 0 and 268 sccm. Gas flow rates were controlled with calibrated mass flow controllers (Tylan General, Rancho Dominguez, CA). Experiment times varied between 15 and 95 h.

Cr Analysis. Care was taken to analyze Cr from all of the vapor products formed in the reaction cell. This involved careful collection and analysis of the deposits in the condensation tubes and the water in the collection burette shown in Figure 2. Several types of deposits were found in the collection tubes: liquid brown deposits and solid green deposits. The identification of these deposits will be discussed in the results section. To collect the deposited Cr for analysis, the fused quartz condensation tubes were injected in succession with deionized water, concentrated HCl, and concentrated HF. Each solvent was left in the tube for about 30 min before flushing with the next solvent. After a final deionized water flush, all solvents were collected in the same beaker, heated, and diluted to a known volume.

The brown and green deposits adhering to the inner walls of the tubes were dislodged by attack of the HF on the fused quartz. Heating the collected solvents dissolved the brown deposit but not the green deposit. The green deposit was filtered off, and the filter paper was transferred to a platinum crucible. The residue was ignited in a muffle furnace at 923 K for 1 h, and then fused in a mixture of 0.9 g anhydrous sodium carbonate and 0.1 g sodium tetraborate at around 1073 K for 10–15 min. When the melt was clear, the crucible was removed from heating and the solidified melt dissolved in deionized water. The solution was then acidified with concentrated HCl and diluted to a known volume. The product of the fusion process was added to the other washings.

The solutions described above, as well as the collected water, were analyzed separately for total Cr by inductively coupled plasma-atomic emission spectrometry (ICP-AES) (Varian Vista Pro Axial View Spectrometer, Varian, Inc.). The collected water from each experiment was also analyzed for hexavalent Cr by a spectrophotometric technique (Shimadzu Model UV-160 Ultraviolet–visible Spectrophotometer, Shimadzu Corp) using 1,5 diphenylcarbohydrazide. The 1,5 diphenylcarbohydrazide reacts with Cr(VI) to develop a vivid pink-purple color that allows the concentration to be determined by measuring the absorbance at 540 nm. This technique verified that the Cr was present in the hexavalent state and, in addition, provided independent confirmation of ICP-AES accuracy.

Theoretical Results and Discussion

The optimum B3LYP/6-311++G(d,p) geometry for CrO₂(OH)₂ has C₂ symmetry. The bond distances are $r(\text{Cr}=\text{O}) = 1.560 \text{ \AA}$, $r(\text{Cr}-\text{O}) = 1.759 \text{ \AA}$, and $r(\text{O}-\text{H}) = 0.967 \text{ \AA}$. The chromium-oxygen bond angles are $\angle\text{O}=\text{Cr}=\text{O} = 111.4^\circ$, $\angle\text{O}-\text{Cr}-\text{O} = 109.9^\circ$, and $\angle\text{O}-\text{Cr}=\text{O} = 110.0^\circ$, 107.8° . The $\angle\text{Cr}-\text{O}-\text{H}$ angle is 116.4° , and the two O–H bonds lie on opposite

TABLE 3: B3LYP/6-311++G(d,p) Frequencies (cm⁻¹) for CrO₂(OH)₂^a

O–Cr–O, O=Cr–O, O=Cr=O bend	Cr–O stretch	Cr–O–H bend	Cr=O stretch	O–H stretch
225(A), 269(A), 294(B), 323(B), 406(A)	734(A), 734(B)	763(A), 785(B)	1083(A), 1107(B)	3810(B), 3815(A)

^a The symmetry of each mode is given in parentheses. In addition to the modes included in the table, there were two modes, at 346(A) and 367(B) cm⁻¹, which were assigned as O–H internal rotations.

TABLE 4: Computation of $\Delta H_{f,0}^\circ$ and $\Delta H_{f,298.15}^\circ$ for CrO₂(OH)₂ from Reaction 5^a

$\Delta E_e[\text{HF}]$	241.98
$\delta[\text{MP2}]$	-2.87
$\delta[\text{CCSD}]$	-13.13
$\delta[\text{CCSD(T)}]$	+0.83
$\delta[\text{core}]$	+1.11
$\delta[\text{basis}]$	-8.45
$\delta[\text{rel}]$	+11.97
$\delta[\text{ZPVE}]$	-9.61
$\Delta H_{f,0}^\circ$	221.83
$\Delta H_{f,0}^\circ[\text{CrO}_2(\text{OH})_2]$	-780.3
$\Delta H_{f,298.15}^\circ[\text{CrO}_2(\text{OH})_2]$	-791.8

^a All entries in kJ mol⁻¹. $\Delta E_e[\text{HF}]$ is the reaction energy computed at the Hartree–Fock level with the Bauschlicher ANO basis set on Cr and the cc-pVTZ set on H and O. $\delta[\text{MP2}]$, $\delta[\text{CCSD}]$, and $\delta[\text{CCSD(T)}]$ designate the changes in the reaction energy relative to the preceding level of theory. $\delta[\text{core}]$, $\delta[\text{basis}]$, $\delta[\text{rel}]$, and $\delta[\text{ZPVE}]$ represent the corrections to the reaction energy from core-correlation, basis set improvement, scalar relativistic effects, and zero-point vibrational energy. $\Delta H_{f,0}^\circ[\text{CrO}_2(\text{OH})_2]$ and $\Delta H_{f,298.15}^\circ[\text{CrO}_2(\text{OH})_2]$ are computed from $\Delta H_{f,0}^\circ$ as described in the text.

sides of the O–Cr–O plane with O–Cr–O–H dihedral angles of -92.4° . The computed harmonic vibrational frequencies and their assignments are given in Table 3. The B3LYP/6-311++G(d,p) structure and frequencies for CrO₂(OH)₂ are similar to previously computed B3LYP values⁸ obtained with a triple- ζ basis set including diffuse functions and a single set of polarization functions on H and O, although our Cr–O and Cr=O bond distances are 0.005–0.006 Å shorter, probably due mainly to inclusion of polarization functions on Cr.

The computation of the heat of formation for CrO₂(OH)₂ from reaction 5 is detailed in Table 4. The HF → MP2, MP2 → CCSD, and CCSD → CCSD(T) increments in the reaction energy are labeled $\delta[\text{MP2}]$, $\delta[\text{CCSD}]$, and $\delta[\text{CCSD(T)}]$, respectively. The small size of these increments, and in particular the $\delta[\text{CCSD(T)}]$ value of only 0.8 kJ mol⁻¹, indicates rapid convergence of the computed reaction energy with respect to improving the treatment of electron correlation. These results lend confidence in the adequacy of the CCSD(T) method, the highest level of electron correlation employed, for computing the reaction energy for reaction 5. The various corrections applied to the computed CCSD(T) reaction energy, $\delta[\text{core}]$, $\delta[\text{basis}]$, and $\delta[\text{rel}]$, assume values of 1.1, -8.5, and 12.0 kJ mol⁻¹. Our final ab initio values for the heat of formation for CrO₂(OH)₂ are $\Delta H_{f,0}^\circ(\text{CrO}_2(\text{OH})_2) = -780 \pm 20 \text{ kJ mol}^{-1}$ and $\Delta H_{f,298.15}^\circ(\text{CrO}_2(\text{OH})_2) = -792 \pm 20 \text{ kJ mol}^{-1}$. The uncertainty of $\pm 20 \text{ kJ mol}^{-1}$ takes into account the reported uncertainties in the employed experimental data and the estimated residual errors in the computation of the reaction energy for reaction 5. Our $\Delta H_{f,298.15}^\circ$ value agrees well with the value of $-787 \pm 36 \text{ kJ mol}^{-1}$ computed previously by Espelid et al.⁸ This may be somewhat fortuitous, however, because their value was obtained by averaging two widely differing numbers (-762 and -812 kJ mol^{-1}) computed using variants of the G2

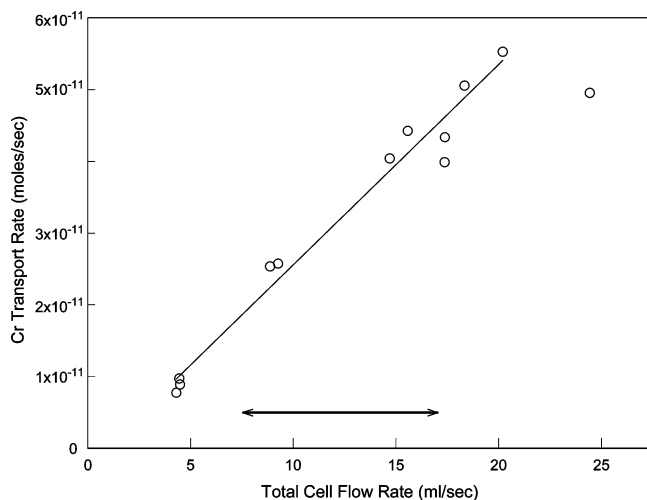


Figure 3. Amount of Cr transported as a function of total transpiration cell flow rate at 873 K, $P(\text{H}_2\text{O}) = 0.08$ and $P(\text{O}_2) = 0.92$. The linear relationship demonstrates the attainment of equilibrium in the transpiration cell. The arrow shows the range of flow rates used during the pressure- and temperature-dependent studies.

extrapolation procedure and the PCI-X method for extrapolating correlation energies. Espelid et al. obtained their heats of formation by computing bond dissociation energies. This approach has a considerable degree of uncertainty when applied to chromium compounds in which the metal is in a high oxidation state. Thus, even though high-level theoretical methods were employed by Espelid et al., the two computed values differ so significantly that a rather large uncertainty must be associated with their reported value.

Experimental Results

The Nature of the Cr Deposits. The $\text{CrO}_2(\text{OH})_2(\text{g})$ condensed in several forms. At temperatures of 873 K and below, a brown liquid chromic acid was found primarily in the horizontal collection tube. The hexavalent state of the brown deposit was confirmed by the spectrophotometric technique as described previously. At higher temperatures, 973 to 1173 K, a green deposit was found in the vertical collection tube in addition to the brown deposit in the horizontal collection tube. The green deposit was analyzed by X-ray diffraction and found to be Cr_2O_3 . It has been observed previously that Cr_2O_3 deposits were found from volatiles formed at 1373 and 1473 K in wet oxygen.⁹ In addition, it has been noted that at 673 K and higher, chromium(VI) oxide decomposes to chromium(III) oxide⁴² so that the condensation of Cr_2O_3 from $\text{CrO}_2(\text{OH})_2(\text{g})$ at higher temperatures seems reasonable.

Attainment of Equilibrium in Transpiration Experiments.

The temperature and pressure dependence of chromia volatility were measured under a range of total flow rates in the transpiration cell, 7.55 to 17.04 mL/s. To make certain that equilibrium was obtained in the transpiration cell, the amount of Cr transported was measured at 873 K, $P(\text{H}_2\text{O}) = 0.08$ and $P(\text{O}_2) = 0.92$ over a wider flow rate range of 4.5 to 24.9 mL/s. As shown in Figure 3, it was found that the amount of Cr transported was proportional to the flow rate up to a rate of 20 mL/s, demonstrating that thermodynamic equilibrium was attained in the cell.

Pressure Dependence of Volatile Species. Because of the uncertainty in the identity of the volatile species in the temperature range of 573 to 1173 K, as well as the temperature ranges under which the previously available experimental data were obtained, $T < 458$ K or $T > 1373$ K, the pressure

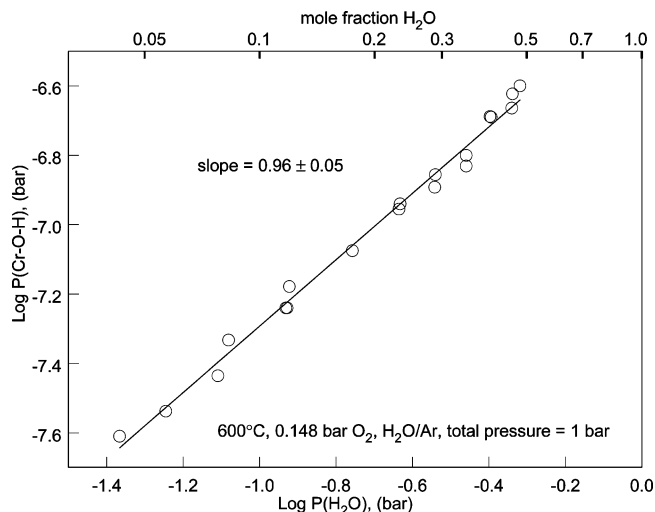


Figure 4. Water-vapor dependence for $\text{Cr}_2\text{O}_3(\text{s})$ volatility obtained at 873 K and constant oxygen partial pressure of 0.15 bar.

dependence of Cr-O-H volatile species formation was determined in this study at 873 K. This temperature was chosen for several reasons. First, at 873 K volatility rates were high enough to measure significant amounts of Cr transport. Second, the temperature was low enough that chromic acid deposits were formed rather than Cr_2O_3 , thus avoiding the more difficult dissolution of the chromium(III) oxide for analysis. Third, this temperature is approximately the midrange temperature of this study. Finally, the volatilization mechanism at this temperature is relevant for the technological applications mentioned previously.

The pressure of volatile Cr-O-H species, $P_{\text{Cr-O-H}}$, was determined using the following expression

$$P_{\text{Cr-O-H}} = \frac{\dot{n}_{\text{Cr}} RT_{\text{cell}}}{\dot{V}} \quad (8)$$

where \dot{n}_{Cr} is the rate of moles of Cr transported, R is the ideal gas constant, T_{cell} is the temperature in the transpiration cell, and \dot{V} is the total flow rate in the transpiration cell. Here \dot{n}_{Cr} and \dot{V} are determined as follows

$$\dot{n}_{\text{Cr}} = \frac{m_{\text{Cr}}}{M_{\text{Cr}} t} \quad (9)$$

where m_{Cr} is the mass of transported Cr as determined by ICP, typically on the order of tens to hundreds of micrograms for a single experiment, M_{Cr} is the molar mass of chromium, and t is the experiment time. In addition

$$\dot{V} = \frac{RT_{\text{cell}}}{P_{\text{tot}}} (\dot{n}_{\text{O}_2} + \dot{n}_{\text{Ar}} + \dot{n}_{\text{H}_2\text{O}} + \dot{n}_{\text{Cr-O-H}}) \quad (10)$$

Here P_{tot} is the total pressure as monitored by the capacitance manometer (typically one bar) and \dot{n}_x are the molar flow rates of oxygen, argon, water, and the volatile species, respectively. The quantity $\dot{n}_{\text{Cr-O-H}}$ is negligible compared to $(\dot{n}_{\text{O}_2} + \dot{n}_{\text{Ar}} + \dot{n}_{\text{H}_2\text{O}})$. Note that the determination of $P_{\text{Cr-O-H}}$ makes no assumptions about the particular vapor species formed except that there is one gas molecule per Cr atom.

The water vapor and oxygen pressure dependencies of the $P_{\text{Cr-O-H}}$ species were determined at 873 K. The $P(\text{H}_2\text{O})$ dependence was determined at a fixed $P(\text{O}_2)$ and is shown in Figure 4. The $P(\text{O}_2)$ dependence was determined at a fixed $P(\text{H}_2\text{O})$ and is shown in Figure 5. It was found that $P_{\text{Cr-O-H}}$

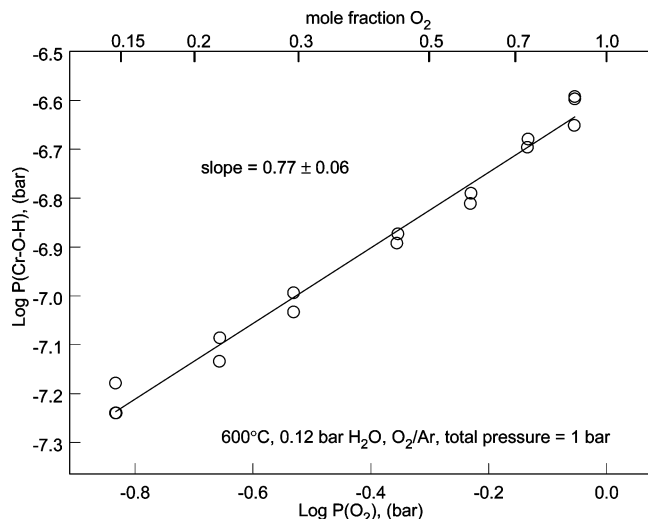


Figure 5. Oxygen dependence for $\text{Cr}_2\text{O}_3(\text{s})$ volatility obtained at 873 K and constant water vapor partial pressure of 0.12 bar.

depended on $P(\text{H}_2\text{O})^n$ and $P(\text{O}_2)^m$ where the power law exponents were $n = 0.96 \pm 0.05$ and $m = 0.77 \pm 0.06$. The reported uncertainties are 95% confidence intervals. These exponents are in excellent agreement with those predicted by reaction 2, $n = 1$ and $m = 3/4$, indicating that $\text{CrO}_2(\text{OH})_2(\text{g})$ is the volatile species formed from the reaction of water vapor and oxygen with Cr_2O_3 at 873 K.

Calculation of Equilibrium Constants for $\text{CrO}_2(\text{OH})_2(\text{g})$ Formation. For each experiment conducted for a time, t , a known amount of oxygen and water vapor flowed through the transpiration cell. The total weight of chromium collected in that same time, t , was determined by ICP analysis. From these three quantities, the equilibrium constant, K_p , for reaction 2 was determined for each experiment as follows

$$K_p = \frac{P_{\text{CrO}_2(\text{OH})_2}}{(a_{\text{Cr}_2\text{O}_3})^{0.5}(X_{\text{H}_2\text{O}}P_{\text{tot}})(X_{\text{O}_2}P_{\text{tot}})^{0.75}} \quad (11)$$

where $P_{\text{CrO}_2(\text{OH})_2}$ is the partial pressure of $\text{CrO}_2(\text{OH})_2(\text{g})$ given by eq 8, P_{tot} is the total pressure measured by the capacitance manometer, and $a_{\text{Cr}_2\text{O}_3}$ is the activity of chromia. By definition, $a_{\text{Cr}_2\text{O}_3}$ equals one assuming the Cr_2O_3 remains pure. X is the mole fraction of a particular gas species, for example, given here for water vapor:

$$X_{\text{H}_2\text{O}} = \frac{\dot{n}_{\text{H}_2\text{O}}}{(\dot{n}_{\text{O}_2} + \dot{n}_{\text{Ar}} + \dot{n}_{\text{H}_2\text{O}} + \dot{n}_{\text{Cr-O-H}})} \quad (12)$$

Heats of Reaction and Formation for $\text{CrO}_2(\text{OH})_2(\text{g})$. Equilibrium constants for reaction 2 were determined for each experiment. The temperature-dependent data are plotted as the log of the equilibrium constant versus $1/T$ in Figure 6. This enables one to determine the second law enthalpy and entropy change for the reaction by means of the well-known van't Hoff relation

$$\frac{\partial \ln K_p}{\partial(1/T)} = -\frac{\Delta H_r^\circ}{R} \quad (13)$$

which upon integration yields

$$\ln K_p = -\frac{\Delta H_r^\circ}{R} \left(\frac{1}{T}\right) + \frac{\Delta S_r^\circ}{R} \quad (14)$$

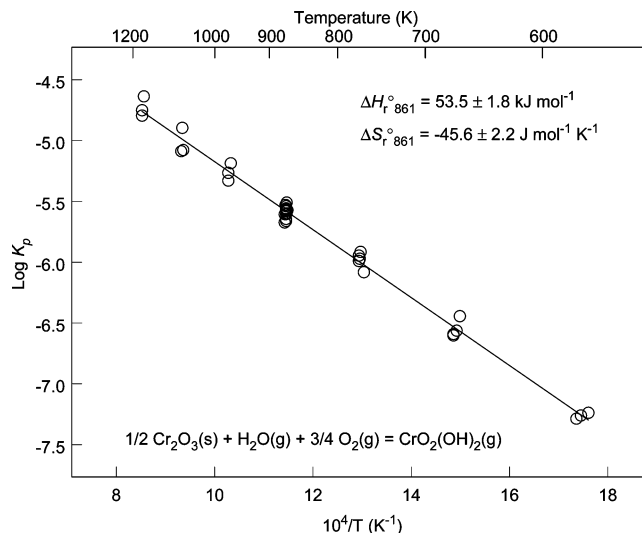


Figure 6. Second law results, ΔH_r° and ΔS_r° and their statistical uncertainty obtained for reaction 2 at an average experimental temperature of 861 K.

The results of this study, obtained at an average temperature of 861 K, yield $\Delta H_{r,861}^\circ = 53.5 \pm 1.8 \text{ kJ mol}^{-1}$. This reported uncertainty is at the 95% confidence level and is a statistical uncertainty from least-squares fitting. However, second law enthalpies are difficult quantities to evaluate reliably due to systematic errors typically associated with accurate temperature control and measurement. Transpiration measurements on a standard sample of known thermochemical properties using the same apparatus have not been made; thus, we have increased the overall uncertainty by a factor of 3 for all reported second law values. As a result, we report a value of $\Delta H_{r,861}^\circ = 53.5 \pm 5.4 \text{ kJ mol}^{-1}$ for reaction 2. This level of uncertainty seems reasonable based on our previous work using the same apparatus to study the $\text{SiO}_2/\text{H}_2\text{O}$ system where other reliable data exist for comparison to our measurements.⁴³ The second law values for the heat of reaction 2 at 298 K were determined from $\Delta H_{r,861}^\circ$ using the heat capacity functions for $\text{CrO}_2(\text{OH})_2$ calculated by ab initio techniques in this work and the heat capacity given by Ebbinghaus¹ both in combination with the heat capacities for $\text{Cr}_2\text{O}_3(\text{s})$, $\text{H}_2\text{O}(\text{g})$, and $\text{O}_2(\text{g})$ from IVTAN-THERMO.¹⁶ The heat capacities for $\text{CrO}_2(\text{OH})_2(\text{g})$ from Ebbinghaus and the ab initio technique in this work are in good agreement, resulting in $\Delta H_{r,298}^\circ = 52.5 \pm 5.4$ and $52.6 \pm 5.4 \text{ kJ mol}^{-1}$ respectively.

The third law heat of reaction can be calculated using Gibbs energy functions.⁴⁴ The Gibbs energy function, gef_T , is defined as

$$gef_T = (G_T^\circ - H_{298}^\circ)/T \quad (15)$$

The third law heat of reaction at 298 K can then be determined from the gef_T and the measured equilibrium constant:

$$\frac{\Delta H_{r,298}^\circ}{T} = -R \ln K_p - \Delta gef_T \quad (16)$$

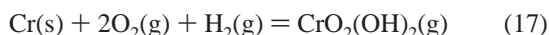
Two sets of theoretical gef functions for $\text{CrO}_2(\text{OH})_2(\text{g})$ were used to calculate a third law enthalpy of reaction: those from the ab initio calculations as well as those estimated by Ebbinghaus.¹ The calculated third law results for each data point are shown in Table 5. Using the ab initio calculated gef of this study yields $\Delta H_{r,298}^\circ = 36.1 \pm 2.7 \text{ kJ mol}^{-1}$ while the gef from Ebbinghaus¹ results in $\Delta H_{r,298}^\circ = 70.9 \pm 3.6 \text{ kJ mol}^{-1}$. The

TABLE 5: Calculated Third Law Results for the Reaction $1/2\text{Cr}_2\text{O}_3(\text{s}) + \text{H}_2\text{O}(\text{g}) + 3/4\text{O}_2(\text{g}) = \text{CrO}_2(\text{OH})_2(\text{g})$ Based on Experimental Data and *gef* from This Study and Ebbinghaus¹

run no.	temp (K)	log K_p	Δ_{gef} (J mol ⁻¹ K ⁻¹) this study	$\Delta H_{\text{f},298}^\circ$ (J mol ⁻¹) <i>gef</i> , this study	Δ_{gef} (J mol ⁻¹ K ⁻¹) Ebbinghaus ¹	$\Delta H_{\text{f},298}^\circ$ (J mol ⁻¹) Ebbinghaus ¹ <i>gef</i>
51	568	-7.2388	66.2643	41077.4	25.91498	63995.8
44	573	-7.2608	66.2744	41675.0	25.90951	64804.1
55	576	-7.2882	66.2803	42192.0	25.90616	65447.5
35	667	-6.4451	66.4070	38007.1	25.78453	65102.3
34	670	-6.5646	66.4095	39709.6	25.77997	66931.3
33	673	-6.5924	66.4118	40243.5	25.77537	67591.8
43	673	-6.6040	66.4118	40393.5	25.77537	67741.8
37	767	-6.0836	66.4336	38376.3	25.61941	69680.8
36	771	-5.9161	66.4326	36104.5	25.61237	67576.9
48	772	-5.9730	66.4323	36993.3	25.61061	68507.7
21	773	-5.9473	66.4320	36660.7	25.60884	68217.0
31	773	-5.9913	66.4320	37311.6	25.60884	68867.8
25	871	-5.5728	66.3685	35118.5	25.43035	70775.7
19	872	-5.5105	66.3676	34119.7	25.42849	69818.6
23	872	-5.5653	66.3676	35034.7	25.42849	70733.6
24	872	-5.5982	66.3676	35584.1	25.42849	71283.0
26	872	-5.5807	66.3676	35292.7	25.42849	70991.6
15	873	-5.5691	66.3667	35139.6	25.42663	70880.3
17	873	-5.5584	66.3667	34960.6	25.42663	70701.3
27	873	-5.5823	66.3667	35359.8	25.42663	71100.5
28	873	-5.5409	66.3667	34669.0	25.42663	70409.7
29	873	-5.6077	66.3667	35785.1	25.42663	71525.8
30	873	-5.6625	66.3667	36700.1	25.42663	72440.8
47	873	-5.6466	66.3667	36435.6	25.42663	72176.3
14	874	-5.5320	66.3658	34559.2	25.42477	70341.7
38	875	-5.6748	66.3649	36992.9	25.42291	72817.2
39	875	-5.6076	66.3649	35866.8	25.42291	71691.0
40	968	-5.1885	66.2853	31988.5	25.24893	71711.7
20	973	-5.2678	66.2820	33634.8	25.23957	73569.1
46	973	-5.3315	66.2820	34821.5	25.23957	74755.8
49	1068	-5.0789	65.3719	34027.5	25.04973	77091.5
41	1070	-4.8973	65.3336	30403.7	25.04774	73519.6
53	1073	-5.0887	65.2746	34492.8	25.04475	77659.4
42	1168	-4.6383	62.0723	31215.3	24.94502	74580.0
50	1173	-4.7522	61.8159	34208.5	24.93955	77464.4
52	1173	-4.7966	61.8159	35205.9	24.93955	78461.8
average	861			36121.4		70860.1
SD				2728.69		3595.28

reported uncertainty is at the 95% confidence level. Note that the calculated third law values should show random scatter but here some temperature dependence is observed that will be discussed below.

The standard heat of formation for CrO₂(OH)₂(g) from the elements is given by the following reaction:



The standard heat of formation was determined using our measured enthalpy of reaction (reaction 2) and the thermodynamic data for Cr₂O₃ and H₂O from IVTANTHERMO.¹⁶ All enthalpies of reaction and formation determined in this study are summarized in Table 6.

Entropy of Reaction and Absolute Entropy of CrO₂(OH)₂(g). The entropy of reaction was determined from the second law analysis as $\Delta S_{\text{r},861}^\circ = -45.6 \pm 2.2 \text{ J mol}^{-1} \text{ K}^{-1}$ as shown in Figure 6. The statistical uncertainty in this value was determined at the 95% confidence level. However, consistent with the enthalpy of reaction, the statistical uncertainty was multiplied by a factor of 3 due to the large uncertainty of the second law method. The second law value of $\Delta S_{\text{r},861}^\circ$ was used to determine S_{861}° and S_{298}° for CrO₂(OH)₂

$$S_{861}^\circ = \Delta S_{\text{r},861}^\circ + 1/2 S^\circ(\text{Cr}_2\text{O}_3, \text{c}) + S^\circ(\text{H}_2\text{O}, \text{g}) + 3/4 S^\circ(\text{O}_2, \text{g}) \quad (18)$$

TABLE 6: Summary of the Enthalpies of Reaction and Formation of CrO₂(OH)₂(g) Determined in This Study

method	$\Delta H_{\text{r},298}^\circ$ (kJ mol ⁻¹), reaction 2	$\Delta H_{\text{f},298}^\circ$ (kJ mol ⁻¹), reaction 17
second law experiment:	53.5 ± 5.4 (861 K)	-758 ± 7 (861 K)
C_p , this study	52.6 ± 5.4 (298 K)	-760 ± 7 (298 K)
Ebbinghaus ¹ C_p	52.5 ± 5.4 (298 K)	-760 ± 7 (298 K)
third law: experiment and <i>gef</i>	36.1 ± 2.7	-776 ± 6
calculated in this study		
third law: experiment and Ebbinghaus ¹ <i>gef</i>	70.9 ± 3.6	-741 ± 6
ab initio calculation CCSD(T)	20.3 (861 K)	-792 ± 20 ^a

^a Calculated from reaction 5.

using the data for Cr₂O₃(c), H₂O(g), and O₂(g) from IVTANTHERMO¹⁶ and

$$S_{298}^\circ = S_{861}^\circ - (S_{861}^\circ - S_{298}^\circ) \quad (19)$$

where the value of the term in parentheses ($S_{861}^\circ - S_{298}^\circ$) is from the theoretical calculations for CrO₂(OH)₂(g) in this study. All calculated values are shown in Table 7 along with data available from other sources for comparison.

Discussion of Experimental Results

Identification of CrO₂(OH)₂(g). The conclusive identification of volatile Cr–O–H species at 873 K as CrO₂(OH)₂(g) was made from the oxygen and water vapor-pressure dependence conducted in this study. We believe this to be valid over the entire temperature range of this study, 573 to 1173 K, for a number of reasons. First, the temperature dependence for reaction 2 (Figure 6) shows a very linear result over the full temperature range, indicating no measurable change in the volatility mechanism. Second, we conducted a transpiration experiment in dry oxygen alone at 1173 K to determine if significant volatility of CrO₃(g) (reaction 1) occurred in the course of our experiments. The contribution of CrO₃(g) to the overall Cr₂O₃ volatility is 1% or less at 1173 K. The contribution of CrO₃(g) to the overall Cr₂O₃ volatility is expected to decrease strongly with decreasing temperature based on the relative temperature dependence for CrO₂(OH)₂(g) and CrO₃(g) (Figure 1). Third, based on the results of Kim and Belton,¹² the contribution of CrO₂(OH)(g) (reaction 3) is for the most part negligible under the conditions studied here. Using Kim and Belton's data, the maximum contribution of CrO₂(OH)(g) to the results obtained here is calculated to be 6.5% at 1173 K, 1.6% at 1073 K, and negligible at lower temperatures. This assumes that Kim and Belton correctly interpreted the contributions of all volatile Cr–O–H species to their results obtained at 1572 to 1798 K. They subtracted contributions of CrO₃(g) from their results based on their measurements in dry oxygen; however, the possible mix of volatile Cr–O–H species appears to be very complex at these higher temperatures (see Figure 1).

Temperature Dependence. The data obtained in this study for reaction 2 are compared to those data found in the literature in Figure 7. It is first noted that there is a wide range of measured and predicted values for the volatility of Cr₂O₃ in oxygen and water vapor by the formation of CrO₂(OH)₂(g). The data from IVTANTHERMO¹⁶ are significantly lower than the others and are neglected from further discussion.

The experimental equilibrium constants obtained by Gindorf^{18,19} and Kurokawa²⁰ are both lower than those reported here. There are two likely reasons for this discrepancy. First, in the present investigations it was observed that both the location and the nature of the CrO₂(OH)₂ condensate depended

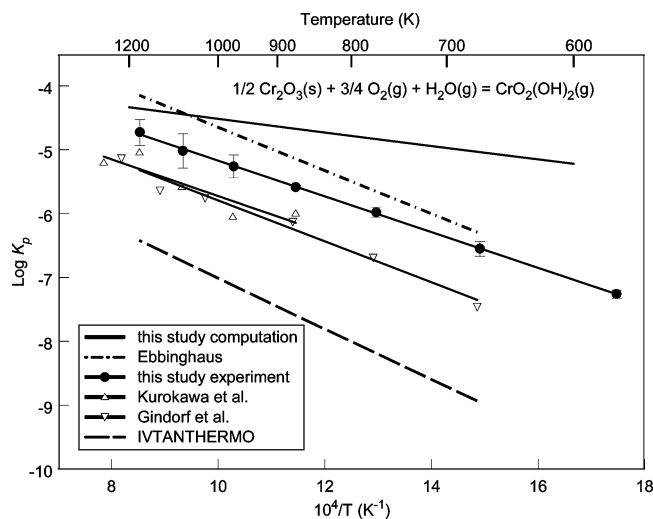


Figure 7. Experimental and computational results from this study for reaction 2 compared to other data found in the literature.

TABLE 7: Summary of Entropies for $\text{CrO}_2(\text{OH})_2(\text{g})$ Formation Determined in This Study Compared to Values Available in the Literature

$\text{J mol}^{-1} \text{K}^{-1}$	$\Delta S_{r,861}^\circ$	S_{861}°	S_{298}°
this study, second law	-45.6 ± 6.6	462.9 ± 8.3	337.6 ± 16.4
this study, theoretical		443.2 ± 10	317.9 ± 10
Ebbinghaus ¹			357.4 ± 4
IVTANTHERMO ¹⁶		$450.1 \pm > 10$	$326.7 \pm > 10$

on the system geometry and temperature. At lower temperatures, significant amounts of Cr were found in the collected water. Also, the Cr_2O_3 deposits formed at temperatures of 973 to 1173 K in this study required a fusion process to dissolve the deposits for analysis. Thus, it is possible that the transported chromium was not completely recovered in previous experiments and was either left in the collected water or incompletely removed from the condensation tubes from high-temperature experiments. Second, both of the previous studies were conducted under a narrow range of conditions of particular interest for fuel cell applications, that is, water vapor contents of 0.02 bar^{18,19} or 0.10 bar²⁰ and oxygen partial pressures of 0.21 bar.^{18–20} In this study, a wider range of water contents (0.05 to 0.5 bar) and oxygen contents (0.15 to 0.95 bar) were assessed. Higher volatility rates and increased sensitivity were thus possible, which increases the accuracy of the measurements.

As mentioned in the introduction, Ebbinghaus¹ estimated data for $\text{CrO}_2(\text{OH})_2(\text{g})$ based on results of Glemser and Mueller¹⁵ obtained at 408 to 458 K for reaction 4. Extrapolating data from such a narrow temperature range to much higher temperatures involves a large degree of uncertainty. Nevertheless, the slopes of the lines in Figure 7 for the experimental studies are similar, indicating somewhat uniform agreement on the temperature dependence of the volatilization by reaction 2. However, the reaction enthalpy for reaction 2, $\Delta H_{r,861}^\circ$, based on the ab initio calculation of $\Delta H_{r,T}^\circ$ is significantly different, 20 kJ mol^{-1} compared to the experimental value of $53.5 \pm 5.4 \text{ kJ mol}^{-1}$.

The analysis of temperature-dependent data by the third law is generally preferred to the second law analysis, given accurate Gibbs energy functions, gef .⁴⁴ In the third law analysis, each data point is evaluated independently of the others and erroneous values can be identified easily. In this case, however, the gef are not accurately known. The gef used in the third law calculations herein were calculated in this study or estimated by Ebbinghaus.¹ Both sets of gef led to calculated third law values of the reaction enthalpy for reaction 2 that vary with the

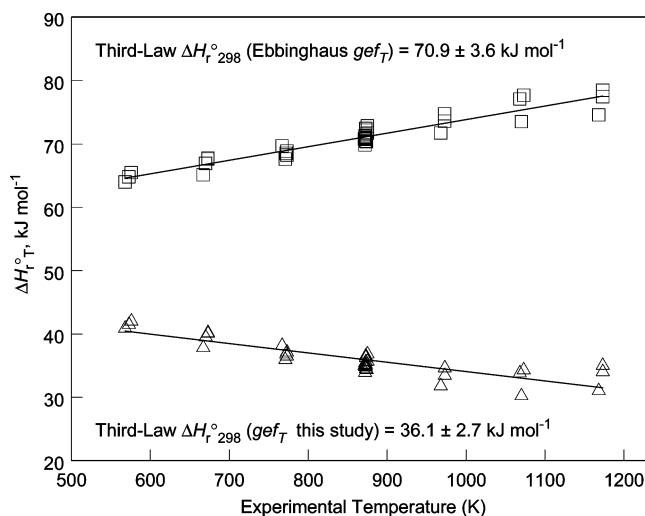


Figure 8. Observed temperature-dependent third law results for $\Delta H_{r,298}^\circ$ obtained from the experimental data and gef s from this study and Ebbinghaus.

experimental temperature as seen in Table 5. This is also shown graphically in Figure 8. The temperature dependence could be due to either systematic errors in the experiments or inaccuracies in the calculated gef . The gef contributes less to the overall calculated third law enthalpies at low temperatures.⁴⁴ For this reason, greater reliance should be placed on the third law values derived from the lower temperature experiments. Note that the third law enthalpies obtained at temperatures near 600 K for both gef are closer to the second law enthalpy value than the third law enthalpies obtained at temperatures near 1200 K. Because of the variation in the third law values, greater confidence is placed in the enthalpy of reaction from the second law value in this particular study. A recent study on the volatilization of chromia-forming alloys showed good agreement between experimental results and results calculated using the second law data from this study,⁴⁵ lending additional confidence to the second law data for $\text{CrO}_2(\text{OH})_2(\text{g})$.

Possible explanations for the discrepancy between the gef computed in this study and by Ebbinghaus as well as explanations for the disagreement between second law and third law values of the reaction enthalpy were sought. The gef from this study were compared to those of Ebbinghaus to try to understand the difference in third law values shown in Figure 8. Most of the difference between the gef of Ebbinghaus and this study is due to the different vibrational frequencies employed, but part of the difference appears to be due to the treatment of hindered rotors. The gef computed in this study are about 38 $\text{J mol}^{-1} \text{K}^{-1}$ below Ebbinghaus'. If the gef are computed using the techniques of this study but using Ebbinghaus' frequencies, geometry, and hindered rotor barrier, a gef is obtained that lies about 13 $\text{J mol}^{-1} \text{K}^{-1}$ below theirs. This residual difference appears to be due to the treatment of the hindered rotation because for molecules without hindered rotors, for example, CrOH, Ebbinghaus' gef can be reproduced using their molecular data and the techniques of this study. Given that the frequencies computed in this study are expected to be significantly more accurate than those employed by Ebbinghaus, the gef computed in this study are recommended over those of Ebbinghaus.

One possible explanation for the observed temperature dependence of the third law values and for the differences between the second and third law results is the presence of anharmonicities in $\text{CrO}_2(\text{OH})_2$ that are not treated accurately. Thus, in $\text{CrO}_2(\text{OH})_2$, in addition to the two hindered rotor modes

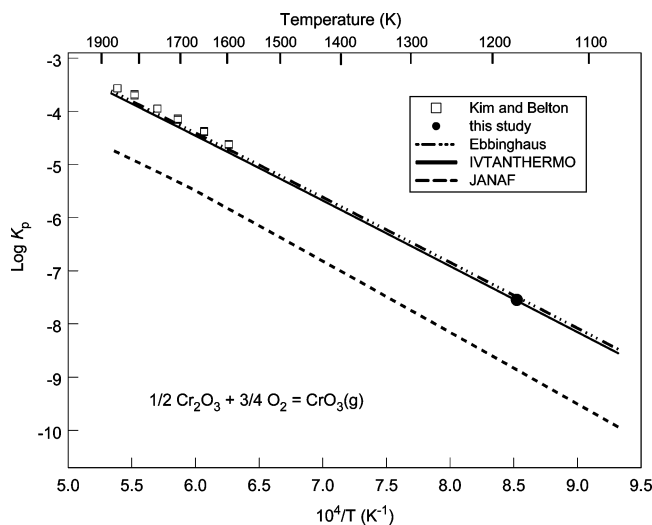


Figure 9. Available data for $\text{CrO}_3(\text{g})$ formation from $\text{Cr}_2\text{O}_3(\text{s})$ in dry oxygen.

at 346 and 367 cm^{-1} , there are four low-frequency modes with computed frequencies of 224, 269, 294, and 323 cm^{-1} . For such low-frequency modes, the harmonic approximation is likely to break down, but, nonetheless, these modes have been treated as harmonic oscillators. We have performed preliminary calculations of thermodynamic functions for $\text{CrO}_2(\text{OH})_2$ to investigate the magnitude of the effect of varying the treatment of the low-frequency modes, using harmonic oscillators, hindered rotors, and free rotors, and the observed effects appear to be sufficiently large to be at least part of the explanation for the problems observed with the third law approach. To our knowledge, no method is currently available for a molecule of this size for doing a proper treatment of low-frequency modes other than internal rotors, and this problem will therefore persist no matter what frequencies are used to compute *gef*. Thus, any computation reported in the literature, for example, Ebbinghaus' result, would have the same problem. We note that if anharmonic effects are the cause for the observed anomalies with the third law approach then greater reliance should be placed on those third law values derived from the lower temperature experiments because anharmonic effects become more pronounced at high temperatures. Unfortunately, there are no data in the literature that we can use to assess the magnitude of anharmonic effects.

$\text{CrO}_3(\text{g})$ Stability. A single control experiment was conducted in dry oxygen at 1173 K in this study to ensure that $\text{CrO}_3(\text{g})$ does not significantly contribute to Cr_2O_3 volatility in oxygen–water vapor mixtures. The experimentally determined pressure of $\text{CrO}_3(\text{g})$ was compared to data available in several databases as shown in Figure 9. It is found that the experimentally determined point from this study is in excellent agreement with Ebbinghaus,¹ the IVTANTHERMO data,¹⁶ and Kim and Belton.¹² The data for $\text{CrO}_3(\text{g})$ available in JANAF²³ differ from the other cited work. The JANAF data²³ are primarily based on mass spectrometric results of Grimley et al.¹⁰ Kim and Belton¹² discuss possible reasons for the lower equilibrium pressures obtained by Grimley. In agreement with IVTANTHERMO, and based on the results shown in Figure 9, the Ebbinghaus data are recommended over those of JANAF. Although the intent of this work was not to study $\text{CrO}_3(\text{g})$, the single experimental result in dry oxygen also gives confidence that our measurement technique is accurate.

$\text{CrO}_2(\text{OH})(\text{g})$ Stability. The new data obtained here for $\text{CrO}_2(\text{OH})_2(\text{g})$ show that lower pressures of this species are predicted

than those based on the estimates of Ebbinghaus.¹ Because of this, Ebbinghaus' estimation of thermodynamic data of $\text{CrO}_2(\text{OH})_2(\text{g})$ must be reevaluated. On the basis of the results of Glemser and Müller¹⁵ for $\text{CrO}_2(\text{OH})_2$, Ebbinghaus concluded that $\text{CrO}_2(\text{OH})_2$, rather than $\text{CrO}_2(\text{OH})$, must be the dominant species Kim and Belton¹² observed in oxygen–water vapor mixtures at temperatures from 1572 to 1798 K. However, now that it has been demonstrated that $\text{CrO}_2(\text{OH})_2(\text{g})$ pressures are lower than those predicted by Glemser and Müller, it appears that Kim and Belton's interpretation of their own data is largely correct. If the results for $\text{CrO}_2(\text{OH})_2(\text{g})$ obtained in the present study at 573 to 1173 K are extrapolated to Kim and Belton's temperature range of 1572 to 1798 K, then it is found that between 80 and 95% of the volatility they observed must be attributed to some species other than $\text{CrO}_2(\text{OH})_2(\text{g})$ or $\text{CrO}_3(\text{g})$. On the basis of their pressure-dependent studies, this other Cr–O–H species was identified as $\text{CrO}_2\text{OH}(\text{g})$. Ebbinghaus states that Kim and Belton did not vary the water and oxygen pressure enough to eliminate the possibility of $\text{CrO}_2(\text{OH})_2(\text{g})$ as the predominant species. Kim and Belton did not report uncertainties in their measured pressure dependence to address this possibility. Therefore, Kim and Belton's results were reanalyzed here to determine uncertainties in their measured pressure dependencies. It was found that $P_{\text{Cr-O-H}}$ depends on $P(\text{H}_2\text{O})^n$ and $P(\text{O}_2)^m$ where the power law exponents were $n = 0.54 \pm 0.24$ and $m = 0.49 \pm 0.11$ at 1572 K and $n = 0.53 \pm 0.11$ and $m = 0.45 \pm 0.13$ at 1677 K. These results are clearly consistent with reaction 3 and statistically different from the power law exponents for reaction 2. Thus Kim and Belton's data for $\text{CrO}_2(\text{OH})(\text{g})$, after correcting for the new thermodynamic data derived here for $\text{CrO}_2(\text{OH})_2(\text{g})$, are preferred over the estimates of Ebbinghaus.

Summary and Conclusions

The transpiration method was used to study the reaction $\frac{1}{2}\text{Cr}_2\text{O}_3(\text{s}) + \text{H}_2\text{O}(\text{g}) + \frac{3}{4}\text{O}_2(\text{g}) = \text{CrO}_2(\text{OH})_2(\text{g})$. It was demonstrated that $\text{CrO}_2(\text{OH})_2(\text{g})$ is the primary vapor species in Cr_2O_3 oxygen water vapor mixtures at 873 K. This is expected to be true to temperatures as high as 1173 K. A heat of formation for $\text{CrO}_2(\text{OH})_2(\text{g})$, $\Delta H_{f,298}^\circ = -792 \pm 20 \text{ kJ mol}^{-1}$, was calculated using high-level ab initio methods. The second law enthalpy and entropy for the reaction $\frac{1}{2}\text{Cr}_2\text{O}_3(\text{s}) + \text{H}_2\text{O}(\text{g}) + \frac{3}{4}\text{O}_2(\text{g}) = \text{CrO}_2(\text{OH})_2(\text{g})$ were found to be $\Delta H_{f,861}^\circ = 53.5 \pm 5.4 \text{ kJ mol}^{-1}$ and $\Delta S_{f,861}^\circ = -45.6 \pm 6.6 \text{ J mol}^{-1} \text{ K}^{-1}$, respectively. The thermodynamic values determined from the second law analysis of the transpiration experimental results are recommended for $\text{CrO}_2(\text{OH})_2(\text{g})$: $\Delta H_{f,298}^\circ = -760 \pm 7 \text{ kJ mol}^{-1}$ and $S_{298}^\circ = 338 \pm 16 \text{ J mol}^{-1} \text{ K}^{-1}$, respectively. Third law analyses of the experimental data showed some temperature dependence of $\Delta H_{f,298}^\circ$ that may be due to inaccuracies in the Gibbs energy functions. The ab initio Gibbs energy functions calculated in this study are expected to be more accurate than those estimated by Ebbinghaus. The discrepancy between the computed heat of formation and the experimental results, as well as the uncertainty associated with the computed Gibbs energy functions, suggest further improvements in ab initio techniques for transition-metal compounds are needed.

At temperatures higher than 1173 K, formation of $\text{CrO}_3(\text{g})$ and $\text{CrO}_2\text{OH}(\text{g})$ are expected to become significant for Cr_2O_3 in environments containing $\text{O}_2(\text{g})$ and $\text{H}_2\text{O}(\text{g})$. The data of Ebbinghaus are recommended for $\text{CrO}_3(\text{g})$. JANAF data for $\text{CrO}_3(\text{g})$ are not recommended. The data of Kim and Belton are recommended for $\text{CrO}_2(\text{OH})(\text{g})$ after correction for the $\text{CrO}_2(\text{OH})_2(\text{g})$ data determined in this study.

Acknowledgment. We thank Tim Gabb (NASA-GRC) for the statistical analysis of Kim and Belton's data and Ralph Garlick (NASA-GRC) for the X-ray diffraction analysis. Funding for this work was provided by Sandia National Laboratories under the U.S. Department of Energy Industrial Materials for the Future Program. Funding for D.M. was provided by the NASA Glenn Research Center under the NASA Summer Faculty Research Opportunities Program.

Supporting Information Available: The computed geometry of the $\text{CrO}_2(\text{OH})_2(\text{g})$ species as well as the computed thermodynamic functions E , H , C_p , S and $(G_T^\circ - H_{298}^\circ)/T$ as a function of temperature between 298.15 and 1000 K. This material is available free of charge via the Internet at <http://pubs.acs.org>.

References and Notes

- (1) Ebbinghaus, B. B. *Combust. Flame* **1993**, *93*, 119.
- (2) Hilpert, K.; Das, D.; Miller, M.; Peck, D. H.; Weiss, R. J. *Electrochem. Soc.* **1996**, *143*, 3642.
- (3) Fergus, J. *Mater. Sci. Eng., A* **2005**, *397*, 271.
- (4) O'Leary, J.; Kunz, R.; von Alten, T. *Environ. Prog.* **2004**, *23*, 194.
- (5) Asteman, H.; Svensson, J.-E.; Johansson, L.-G.; Norell, M. *Ox. Met.* **1999**, *52*, 95.
- (6) Yamauchi, A.; Kurokawa, K.; Takahashi, H. *Ox. Met.* **2003**, *59* (5/6), 517.
- (7) Bailey, J. J. *Electrochem. Soc.* **1997**, *144*, 3568.
- (8) Espelid, Ø.; Børve, K. J.; Jensen, V. R. *J. Phys. Chem. A* **1998**, *102*, 10414.
- (9) Caplan, D.; Cohen, M. J. *Electrochem. Soc.* **1961**, *108*, 438.
- (10) Grimley, R. T.; Burns, R. P.; Inghram, M. G. *J. Chem. Phys.* **1961**, *34*, 664.
- (11) Graham, H. C.; Davis, H. H. *J. Am. Ceram. Soc.* **1971**, *54*, 89.
- (12) Kim, Y.-W.; Belton, G. R. *Met. Trans.* **1974**, *5*, 1811.
- (13) Fryburg, G. C.; Miller, R. A.; Kohl, F. J.; Stearns, C. A. *J. Electrochem. Soc.* **1977**, *124*, 1738.
- (14) Farber, M.; Srivastava, R. D. *Combust. Flame* **1973**, *20*, 43.
- (15) Glemser, O.; Müller, A. Z. *Anorg. Allg. Chem.* **1964**, *334*, 150.
- (16) *IVTANTHERMO* for Windows, version 3.0, 1992–2003.
- (17) Gorokhov, L. N. Personal communication, 2005.
- (18) Gindorf, C.; Singheiser, L.; Hilpert, K. *J. Phys. Chem. Solids* **2005**, *66*, 384.
- (19) Gindorf, C.; Hilpert, K.; Singheiser, L. *Solid Oxide Fuel Cells VII (SOFC VII)*; The Electrochemical Society Proceedings Series, PV2001-16; Electrochemical Society: Pennington, NJ, 2001; p 793.
- (20) Kurokawa, H.; Jacobson, C. P.; DeJonghe, L. C.; Visco, S. J.; Chromium vaporization of uncoated and of coated iron chromium alloys at 1073 K, unpublished work.
- (21) JANAF Thermochemical Tables, 3rd ed.; *J. Phys. Chem. Ref. Data* **1985**, *14* (Suppl. 1).
- (22) Frisch, M. J.; Pople, J. A.; Binkley, J. S. *J. Chem. Phys.* **1984**, *80*, 3265.
- (23) Wachters, A. J. H. *J. Chem. Phys.* **1970**, *52*, 1033.
- (24) Hay, P. J. *J. Chem. Phys.* **1977**, *66*, 4377.
- (25) Comment: For Cr, the 6-311++G(d,p) set is the Wachters–Hay all electron basis using the scaling factors of Raghavachari and Trucks.
- (26) Bauschlicher, C. W. *Theor. Chim. Acta* **1995**, *92*, 183.
- (27) Basislib: obtained from the *Extensible Computational Chemistry Environment Basis Set Database*, version 1/02/02; Molecular Science Computing Facility, Environmental and Molecular Sciences Laboratory, Pacific Northwest Laboratory, P.O. Box 999, Richland, Washington 99352. Funded by the U.S. Department of Energy. Contact David Feller or Karen Schuchardt for further information.
- (28) Dunning, T. H., Jr.; *J. Chem. Phys.* **1989**, *90*, 1007.
- (29) Kendall, R. A.; Dunning, T. H., Jr.; Harrison, R. J. *J. Chem. Phys.* **1992**, *96*, 6796.
- (30) Douglas, M.; Kroll, N. M. *Ann. Phys.* **1974**, *82*, 89.
- (31) Hess, B. A. *Phys. Rev. A* **1985**, *32*, 756.
- (32) Hess, B. A. *Phys. Rev. A* **1986**, *33*, 3742.
- (33) Jansen, G.; Hess, B. A. *Phys. Rev. A* **1989**, *39*, 6016.
- (34) de Jong, W. A.; Harrison, R. J.; Dixon, D. A. *J. Chem. Phys.* **2001**, *114*, 48.
- (35) McQuarrie, D. A. *Statistical Mechanics*; Harper & Row: New York, 1976.
- (36) Pitzer, K. S.; Gwinn, W. D. *J. Chem. Phys.* **1942**, *10*, 428.
- (37) Straatsma, T. P.; Aprà, E.; Windus, T. L.; Bylaska, E. J.; de Jong, W.; Hirata, S.; Valiev, M.; Hackler, M.; Pollack, L.; Harrison, R.; Dupuis, M.; Smith, D. M. A.; Nieplocha, J.; Tipparaju, V.; Krishnan, M.; Auer, A. A.; Brown, E.; Cisneros, G.; Fann, G.; Früchtl, H.; Garza, J.; Hirao, K.; Kendall, R.; Nichols, J.; Tsemekhman, K.; Wolinski, K.; Anshell, J.; Bernholdt, D.; Borowski, P.; Clark, T.; Clerc, D.; Dachsel, H.; Deegan, M.; Dyall, K.; Elwood, D.; Glendenning, E.; Gutowski, M.; Hess, A.; Jaffe, J.; Johnson, B.; Ju, J.; Kobayashi, R.; Kutteh, R.; Lin, Z.; Littlefield, R.; Long, X.; Meng, B.; Nakajima, T.; Niu, S.; Rosing, M.; Sandrone, G.; Stave, M.; Taylor, H.; Thomas, G.; van Lenthe, J.; Wong, A.; Zhang, Z.; NWChem, A Computational Chemistry Package for Parallel Computers Version 4.6 (2004), Pacific Northwest National Laboratory, Richland, Washington, 99352–0999. High Performance Computational Chemistry: an Overview of NWChem a Distributed Parallel Application, Kendall, R. A.; Aprà, E.; Bernholdt, D. E.; Bylaska, E. J.; Dupuis, M.; Fann, G. I.; Harrison, R. J.; Ju, J.; Nichols, J. A.; Nieplocha, J.; Straatsma, T. P.; Windus, T. L.; Wong, A. T. *Comput. Phys. Commun.* **2000**, *128*, 260.
- (38) Janssen, C. L.; Nielsen, I. B.; Leininger, M. L.; Valeev, E. F.; Seidl, E. T. *The Massively Parallel Quantum Chemistry Program (MPQC)*, version 2.3.0-alpha; Sandia National Laboratories, Livermore, CA, 2004.
- (39) Frisch, M. J.; Trucks, G. W.; Schlegel, H. B.; Scuseria, G. E.; Robb, M. A.; Cheeseman, J. R.; Montgomery, J. A., Jr.; Vreven, T.; Kudin, K. N.; Burant, J. C.; Millam, J. M.; Iyengar, S. S.; Tomasi, J.; Barone, V.; Mennucci, B.; Cossi, M.; Scalmani, G.; Rega, N.; Petersson, G. A.; Nakatsuji, H.; Hada, M.; Ehara, M.; Toyota, K.; Fukuda, R.; Hasegawa, J.; Ishida, M.; Nakajima, T.; Honda, Y.; Kitao, O.; Nakai, H.; Klene, M.; Li, X.; Knox, J. E.; Hratchian, H. P.; Cross, J. B.; Bakken, V.; Adamo, C.; Jaramillo, J.; Gomperts, R.; Stratmann, R. E.; Yazyev, O.; Austin, A. J.; Cammi, R.; Pomelli, C.; Ochterski, J. W.; Ayala, P. Y.; Morokuma, K.; Voth, G. A.; Salvador, P.; Dannenberg, J. J.; Zakrzewski, V. G.; Dapprich, S.; Daniels, A. D.; Strain, M. C.; Farkas, O.; Malick, D. K.; Rabuck, A. D.; Raghavachari, K.; Foresman, J. B.; Ortiz, J. V.; Cui, Q.; Baboul, A. G.; Clifford, S.; Cioslowski, J.; Stefanov, B. B.; Liu, G.; Liashenko, A.; Piskorz, P.; Komaromi, I.; Martin, R. L.; Fox, D. J.; Keith, T.; Al-Laham, M. A.; Peng, C. Y.; Nanayakkara, A.; Challacombe, M.; Gill, P. M. W.; Johnson, B.; Chen, W.; Wong, M. W.; Gonzalez, C.; Pople, J. A. *Gaussian 03*, revision A.1; Gaussian, Inc.: Wallingford, CT, 2004.
- (40) Merten, U.; Bell, W. E. The Transpiration Method. In *The Characterization of High Temperature Vapors*; Margrave, J. L., Ed.; John Wiley & Sons, Inc.: NY, 1967; p 91.
- (41) <http://barometer.grc.nasa.gov/cgi-bin/barometer.cgi>.
- (42) Daintith, J. *The Oxford Paperback Reference Dictionary of Chemistry*, 3rd ed.; Oxford University Press: NY, 1996; p 117.
- (43) Jacobson, N. S.; Opila, E. J.; Myers, D. L.; Copland, E. H. *J. Chem. Thermodyn.* **2005**, *37*, 1130.
- (44) Stull, D. R.; Prophet, H. The Calculation of Thermodynamic Properties of Materials over Wide Temperature Ranges. In *The Characterization of High Temperature Vapors*; Margrave, J. L., Ed.; John Wiley & Sons, Inc.: NY, 1967; p 404.
- (45) Young, D. J.; Pint, B. A. *Ox. Met.* **2006**, *66*, 137.